P12.5 SPECTRUM-TIME ESTIMATION AND PROCESSING (STEP) ALGORITHM FOR IMPROVING WEATHER RADAR DATA QUALITY

Qing Cao[1], Guifu Zhang[1,2], Robert D. Palmer[1,2] Ryan May[3], Robert Stafford[3] and Michael Knight[3]

[1]*Atmospheric Radar Research Center, University of Oklahoma, Norman, OK 73072*

[2]*School of Meteorology, University of Oklahoma, Norman, OK 73072*

[3]*Enterprise Electronics Corporation (EEC), Enterprise, AL 36330*

1. INTRODUCTION

Enhanced data quality would improve the application of radar data in various meteorological algorithms. As we know, ground clutter and noise are two major factors that adversely affect the quality of radar data. Ground clutter, which is normally present at low elevation and near range radar observations, heavily biases weather measurements such as power, mean velocity, spectrum width, and polarimetric observables. Noise, another main source of error, limits radar sensitivity of weak weather echoes and causes measurement biases. Therefore, the removal of ground clutter and noise effect is desired to obtain accurate measurement of weather phenomena.

In cooperation with Enterprise Electronics Corporation (EEC), the Atmospheric Radar Research Center (ARRC) at the University of Oklahoma (OU) has developed a Spectrum-Time Estimation and Processing (STEP) algorithm, aiming to improve the quality of polarimetric radar data in the presence of ground clutter and noise. STEP algorithm integrates three novel algorithms recently developed in ARRC, such as Spectrum Clutter Identification (SCI, Li et al. 2011), Bi-Gaussian Clutter Filtering method (BGCF), and the Multi-lag Moment Estimation method (MLAG, Lei et al. 2009, Cao et al. 2010). Accordingly, STEP algorithm consists of three major modules: SCI, BGCF, and MLAG, that fulfill three functions: clutter identification, clutter filtering and moment estimation, respectively. STEP algorithm has been tested using the C-band polarimetric research radar OU-PRIME (University of Oklahoma—Polarimetric Radar for Innovations in Meteorology and Engineering) (Palmer et al. 2011). This paper intends to give an overall introduction of STEP algorithm and demonstrates its performance using simulated and real data.

* Corresponding author address: Qing Cao; 120 David L. Boren Blvd. Suite 4638, Norman, OK 73072, U.S.A.; E-mail: qingcao@ou.edu

2. METHODOLOGY OF STEP ALGORITHM

STEP algorithm includes three major modules as shown in the flowchart in Fig. 1. First, the I/Q data from the horizontal (H) and vertical (V) polarization channels are input into the SCI module (step 1). This module makes the decision on the identification of clutter contamination. If there is clutter contamination, the BGCF module (step 2) will remove the ground clutter in the spectral domain and reconstruct I/Q with the filtered spectrum for moment estimation in the MLAG module (step 3). A complementary function is included in the BGCF module. When the Bi-Gaussian Clutter Filtering method has a slow convergence, or fails to converge, a single-Gaussian clutter filtering method, which is similar to the concept of GMAP, is applied. If there is no clutter contamination, the original I/Q data are conveyed directly to the MLAG module (step 3) to estimate polarimetric parameters.

2.1 Spectrum Clutter Identification (SCI)

Li et al. (2011) recently proposed the spectrum clutter identification algorithm, which uses a fuzzy-logic classification framework with four characteristic inputs, i.e., spectral power discriminant (SPD), spectral phase fluctuation (SPF), power texture (PT), and spectrum width texture (SWT). This algorithm is designed for the application of single-polarization radar data. The details of SCI algorithm can be found in Li et al. (2011). Compared to the clutter mitigation decision (CMD) algorithm developed by the National Center for Atmospheric Research (NCAR), SCI algorithm shows a better probability of detection (POD) and probability of false alarm (PFA), especially for radar echoes with a low clutter-to-signal-ratio (CSR) and those with a Doppler velocity close to zero. The SCI algorithm used in STEP algorithm includes an additional input parameter, i.e., correlation coefficient (ρ_{hv}), for its implementation on polarimetric weather radar. The fuzzy range of ρ_{hv} is chosen from 0.8 to 0.95 in STEP algorithm.

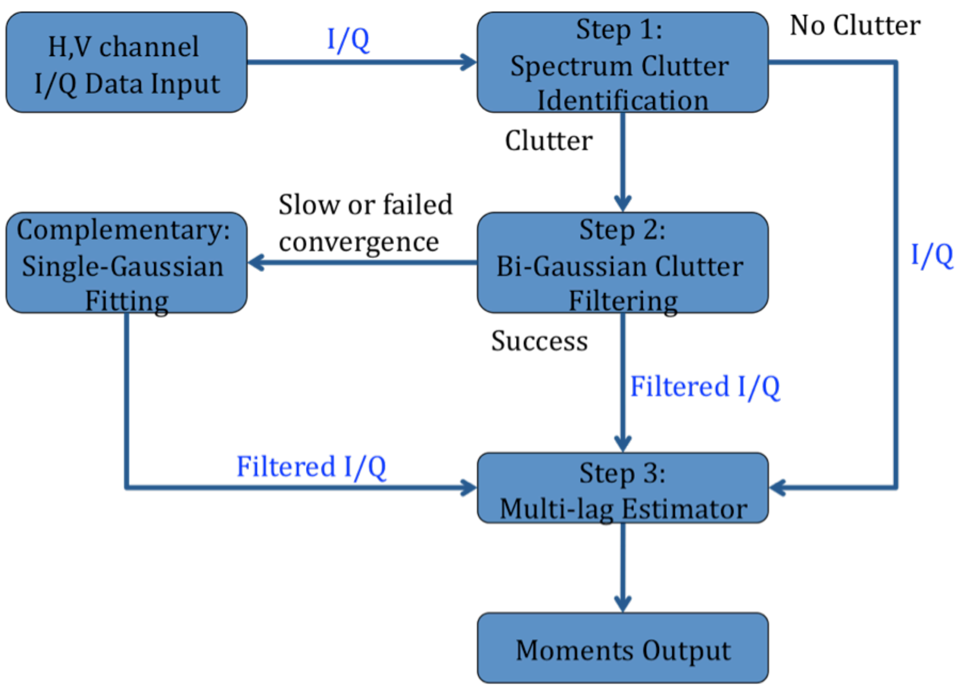

Fig. 1 Flowchart of STEP algorithm

2.2 Bi-Gaussian Clutter Filtering (BGCF)

The BGCF algorithm removes ground clutter in the spectral domain. The fundamental assumption of BGCF is that both weather echoes and ground clutter have a power spectrum of Gaussian shape. The total power spectrum of the radar signal consists of three components: ground clutter, weather signal, and noise; as modeled by

$$S(v) = s_c \exp\left(-\frac{v^2}{2\sigma_c^2}\right) + s_w \exp\left(-\frac{(v - v_w)^2}{2\sigma_w^2}\right) + n_\varepsilon \quad (1)$$

The ground clutter is assumed to have zero mean Doppler velocity, spectrum width σ_c, and maximal power density s_c. The weather signal has mean velocity v_w, spectrum width σ_w, and maximal power density s_w. The noise component has a constant power density n_ε. These unknown parameters are fitted to the observed power spectrum using a standard non-linear fitting algorithm (e.g., Levenberg -Marquardt method). Considering the window effect during the calculation of power spectrum, three aggressive window functions: Blackman-Harris, Blackman, and Hamming windows are applied in STEP according to different signal-to-noise ratios (SNR). As suggested by the 3rd step MLAG, BGCF's output should be converted into time-domain to do the moment estimation. It is noted that the nonlinear fitting using the bi-Gaussian model has separated the contributions of weather signal and clutter to the total power spectrum. The Fourier spectrum of original signal, therefore, can be modified and reconstructed accordingly to remove the clutter portion. The new I/Q data are then calculated through the Inverse Fast Fourier Transform (IFFT) of reconstructed Fourier spectrum, which discards the clutter portion. The phase of clutter-contaminated portion in the spectrum is substituted by random phase to emulate the phase of weather signal.

There are two issues that might affect the real-time implementation of BGCF. The nonlinear regression might have too much iteration before achieving convergence. Moreover, the regression might not be able to converge if the observed spectrum is not well represented by the bi-Gaussian model. In those cases, BGCF applies a complementary fitting approach with a single-Gaussian weather model to solve the problem. The single-Gaussian model only considers the spectrum of weather and noise, as shown in equation (2).

$$S'(v) = s_w \exp\left(-\frac{(v - v_w)^2}{2\sigma_w^2}\right) + n_\varepsilon \qquad (2)$$

The only difference between the fittings using single-Gaussian model or bi-Gaussian model is whether the spectrum lines within clutter bins are applied for the fitting. The fitting approach using single-Gaussian model does not consider those bins and only fits weather and noise spectrum. The range of clutter bins is estimated using an empirical method. A Gaussian curve with a spectrum width of 0.5 m/s is assumed for the clutter spectrum. The amplitude of the Gaussian curve equals the mean power density within the range of ±0.1 m/s. The clutter range is within $\pm v_c$, where v_c denotes the velocity at which the Gaussian curve arrives at the noise floor in the power spectrum.

2.3 Multi-Lag Moment Estimator (MLAG)

The concept of multi-lag processing has been described in Lei et al. (2011). Cao et al. (2010, 2011) have applied an adaptive weighting to fit the auto-correlation function (ACF) and/or cross-correlation function (CCF) of radar signals. The fitted ACF and CCF can then be used to estimate radar variables such as signal power S_h (or S_v), differential reflectivity Z_{DR}, correlation coefficient ρ_{hv}, spectrum width σ_h (or σ_v), differential phase (Φ_{DP}) and radial velocity v_h (or v_v). The MLAG module of STEP algorithm is briefly addressed as follows.

As for weather signals, ACF for horizontal polarization (C_h) and ACF for vertical polarization (C_v) and CCF C_{hv} are all modeled by a Gaussian function C_p (p: h, v, and hv), which is:

$$C_p(m) = C_p(0)\exp\left(-\frac{m^2}{2w_p^2}\right) \qquad (3)$$

where m is the lag number of ACF/CCF; w_p is the decorrelation length of ACF/CCF. The Gaussian ACF/CCF can be fitted through multiple lags of ACF/CCF estimated from I/Q data. The fitting process of MLAG is to minimize the cost function χp as:

$$\chi_p = \sum_{m=1}^{M}\left[C_p(m) - \left|\hat{C}_p(m)\right|\right]^2 C_p(m) \qquad (4)$$

Considering weather signals may decorrelate at farther lags, the cost function in equation (6) applies an adaptive weighting of the Gaussian model itself.

The estimation of radar moments is based on the nonlinear fitted ACF and CCF. The equations are given as follows.

$$S_{h,v} = C_{h,v}(0) \qquad (5)$$

$$Z_{DR} = 10\log_{10}\left[\frac{S_h}{S_v}\right] \text{ (dB)} \qquad (6)$$

$$\sigma_{h,v} = \frac{v_a}{\pi w_{h,v}} \qquad (7)$$

$$\rho_{hv} = \frac{C_{hv}(0)}{\sqrt{C_h(0)C_v(0)}} \quad (8)$$

$$\phi_{DP}(m) = \arg\left[\hat{C}_{hv}(m)\right] - 0.5 \times \left(\arg\left[\hat{C}_h(m)\right] + \arg\left[\hat{C}_v(m)\right]\right) \quad (9.a)$$

$$\Phi_{DP} = \frac{\sum_{m=1}^{w_n} C_{hv}(m) \times \phi_{DP}(m)}{\sum_{m=1}^{w_n} C_{hv}(m)} \quad (9.b)$$

$$v'_{h,v}(m) = \frac{-v_a}{m\pi} \times \arg\left[\hat{C}_{h,v}(m)\right] \quad (10.a)$$

$$v_{h,v} = \frac{\sum_{m=1}^{w_n} C_{hv}(m) \times \mathrm{unwrap}\left[v'_{h,v}(m)\right]}{\sum_{m=1}^{w_n} C_{hv}(m)} \quad (10.b)$$

where w_n is the number of usable lags; the notation "arg[.]" represents the phase of a complex number; the notation "unwrap[.]" means unwrapping the velocity estimation at different lags (m>1). Since the velocity aliasing is different for estimations from different lags of ACF, the unwrapping process is needed before averaging.

It is worth noting that the more usable lags, the better the multi-lag fitting result. The relation between the number of usable lags w_n and spectrum width σ is:

$$w_n = \frac{v_a}{\pi\sigma} = \frac{\lambda}{4T_s\pi\sigma} \quad (11)$$

where λ is the radar wavelength and T_s is the pulse repetition time (PRT). It is obvious that the wider the spectrum width, the lower the usable lag number. For example, the C-band OU-PRIME radar normally operates with a pulse repetition frequency (PRF) of 1180 Hz and its v_a is 16.07 m/s. Given that a weather signal has a spectrum width of 0.5-2 m/s, the usable number is 3-10. For S-band radar, if the conditions are the same, the number of usable lags will be double. Consequently, it is expected that the MLAG algorithm would perform better on S-band over C-band.

3. PERFORMANCE OF STEP ALGORITHM

3.1 Clutter Identification

The clear air observations at low elevation scan (0 or 0.5 degree) are assumed to be the truth of ground clutter. High elevation (3.5 degree) observations of storm, which are less affect by the ground clutter, are assumed to be the truth of weather signals. The storm and clear air time-series I/Q data are coherently combined to simulate the clutter-contaminated weather data for the evaluation. There are total 18 experimental datasets chosen from events of 04/12/2009, 10/21/2009, 12/02/2009, 01/21/2010, 04/17/2010, 04/18/2010, 05/13/2010, 05/14/2010, and 09/08/2010, which all include widespread stratiform precipitation. The clear air data are collected on 08/04/2010 and 01/13/2011. For the comparison, the CMD algorithm is run and evaluated with the same dataset as well.

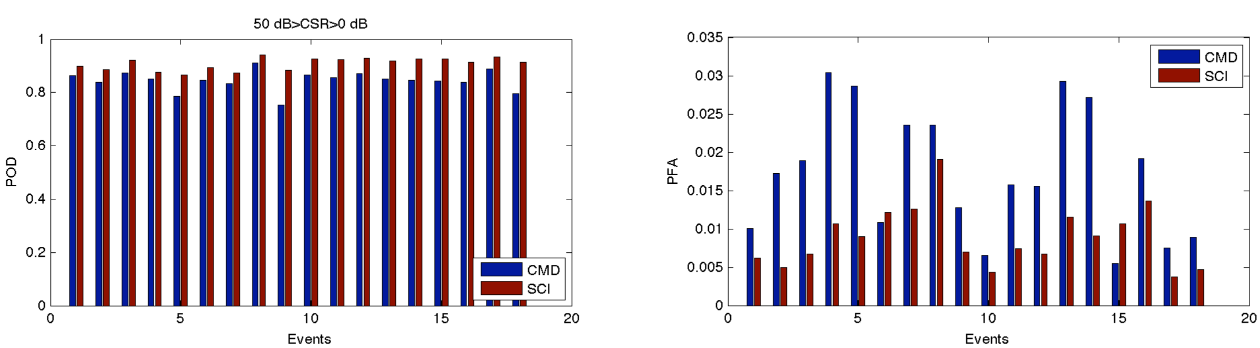

Fig. 2 Comparison of (a) POD and (b) PFA between CMD and SCI algorithms for 18 experimental datasets.

Fig. 2 shows the probability of detection (POD) and probability of false alarm (PFA) of clutter identification results using SCI and CMD algorithms. Clutter truth for cases 1-9 come from clear air observation at 0.5 degrees and the rest cases are for 0 degree observation. SCI generally has higher detection rate and lower false alarm rate than CMD algorithm, which has been widely recognized as a sufficient clutter identifier and has been applied in the NEXRAD network. On average, SCI has POD of 90.8%, greater than CMD's 84.5%, and a low PFA around 0.9%, lower than CMD's 1.73%.

3.2 Clutter Filtering

The performance of BGCF depends on the number of pulses used to estimate the power spectrum. Fig. 3 shows the trend of this dependence. The simulated weather signals have a spectrum width of 2.5 m/s. The CSR is 10 dB. The upper row shows the quantification for weather velocity of 2 m/s and the lower row is for weather velocity of 6 m/s. Solid lines in Fig. 3 denote the bias of BGCF processed moments. The vertical bars indicate the standard deviation of the moment estimation error. As Fig. 3 shows, the BGCF performance is improved with increasing pulse number. This is reasonable because more data points along the power spectrum may lead to an improved fitting. In addition, the lower row shows a better performance than the upper row. This fact implies that fitting a spectrum with weather and clutter components separated out is easier than fitting an overlapped spectrum. It is worth noting that BGCF based on 64 pulses generally performs well. BGCF based on 32 pulses can also function well if the weather and clutter signals are well separated in the spectral domain.

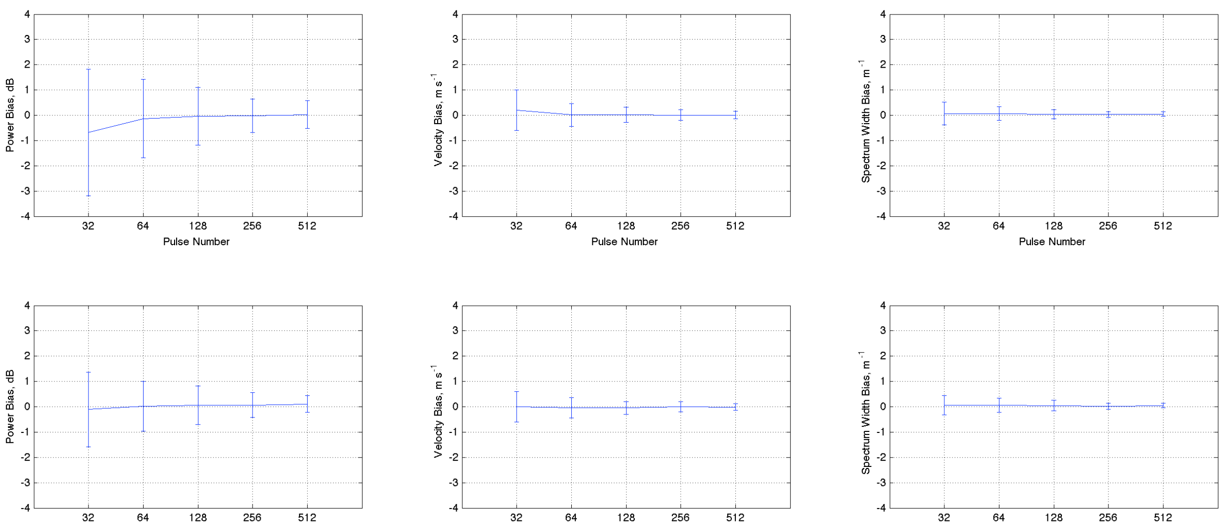

Fig. 3 The effect of pulse number on the bias and error of BGCF processed moments. Three columns from left to right show power, velocity, and spectrum width, respectively. Simulated data have CSR = 10 dB, and weather spectrum width σ = 2.5 m/s. The weather velocity is: (upper row) v = 2 m/s, and (lower row) v = 6 m/s.

The performance of BGCF also depends on the CSR. Fig. 4 shows its quantification and compares BGCF results with the results of the notch filter that is embedded in the signal processor of OU-PRIME, which has a suppression of -50 dB. As Fig. 4 shows, the BGCF method demonstrates superb performance in removing the clutter contamination (much better than traditional notch filter method). The power, velocity and spectrum width estimates have very small bias, especially for CSR < 30 dB. The estimation errors are also minor. For example, as for CSR < 30 dB, the errors of power, velocity, and spectrum width estimations are within 2 dB, 0.7 m/s, and 0.4 m/s, respectively. The notch filter, however, causes a large bias for all three moments. The bias and error of BGCF are insignificant for small to moderate CSRs. When CSR is large, e.g., CSR > 35 dB, BGCF's performance tends to degrade, but still not much. Even for CSR = 60 dB, the power bias is only around 3 dB, though the standard error increases to 9 dB. Fig. 4 also implies that the increase of CSR has little effect on the estimation of velocity and spectrum width.

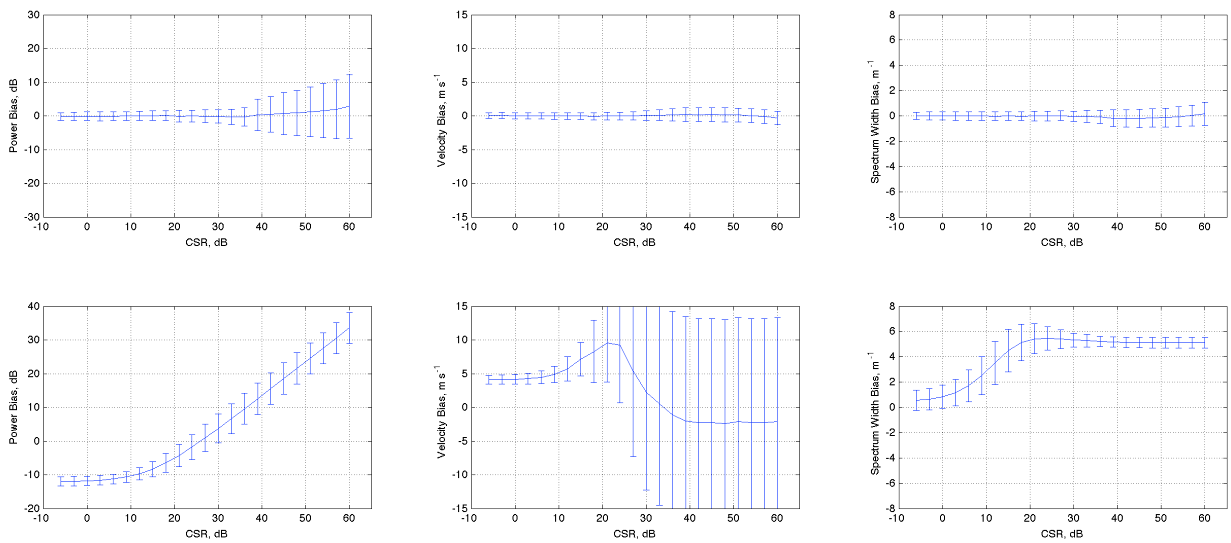

Fig. 4 The effect of CSR on the bias and error of BGCF processed moments. The three columns from left to right show power, velocity, and spectrum width, respectively. Simulated weather data have a spectrum width σ = 2.5 m/s, and a velocity v = 2 m/s. Pulse number is 64. The weather velocity is: (upper row) processing with BGCF, and (lower row) processing with -50 dB notch filter of OU-PRIME.

3.3 Noise Mitigation

MLAG algorithm can improve moment estimation in the presence of noise. The most effective improvements are achieved in estimating power, spectrum width, and correlation coefficient. Cao et al. (2010) have shown the quantification of MLAG algorithm for these three moments. The result shows that MLAG algorithm can effectively improve power, spectrum width and correlation coefficient estimation for SNR < 20dB. The improvement is more evident for low SNRs, e.g., SNR<5 dB. Another advantage of the MLAG method is that it can mitigate the contamination of second trip echoes if the radar applies the magnetron transmitter, which has automatic random phase coding. The details of the second trip mitigation have been specified in Cao et al. (2011) and are not presented here.

4. CASE STUDY OF STEP ALGORITHM

The STEP algorithm has a complete combination of aforementioned advantages from its three modules. This section gives a real data example to demonstrate the superior performance of STEP. Fig. 5 shows a case from 21 October 2009, whose data are combined with the clutter observation on 13 January 2011. Figure 5(b) shows the PPI (plan position indicator) image of CSR. In the image, the pixel with CSR>0 dB is assumed to have clutter contamination. Accordingly, the image of clutter truth is shown in Figure 5(c). Figure 5(a) shows the velocity estimation based on the traditional lag one estimation. It is seen that the clutter-contaminated pixels are biased towards 0 m/s. Figure 5(d) shows the clutter identification result, which has been processed with the STEP algorithm. Comparing the STEP result with the clutter truth, we see that the feature of the clutter region is quite similar for both images. Further comparison shows that the POD of STEP is 97.5% and the PFA is 2.6%.

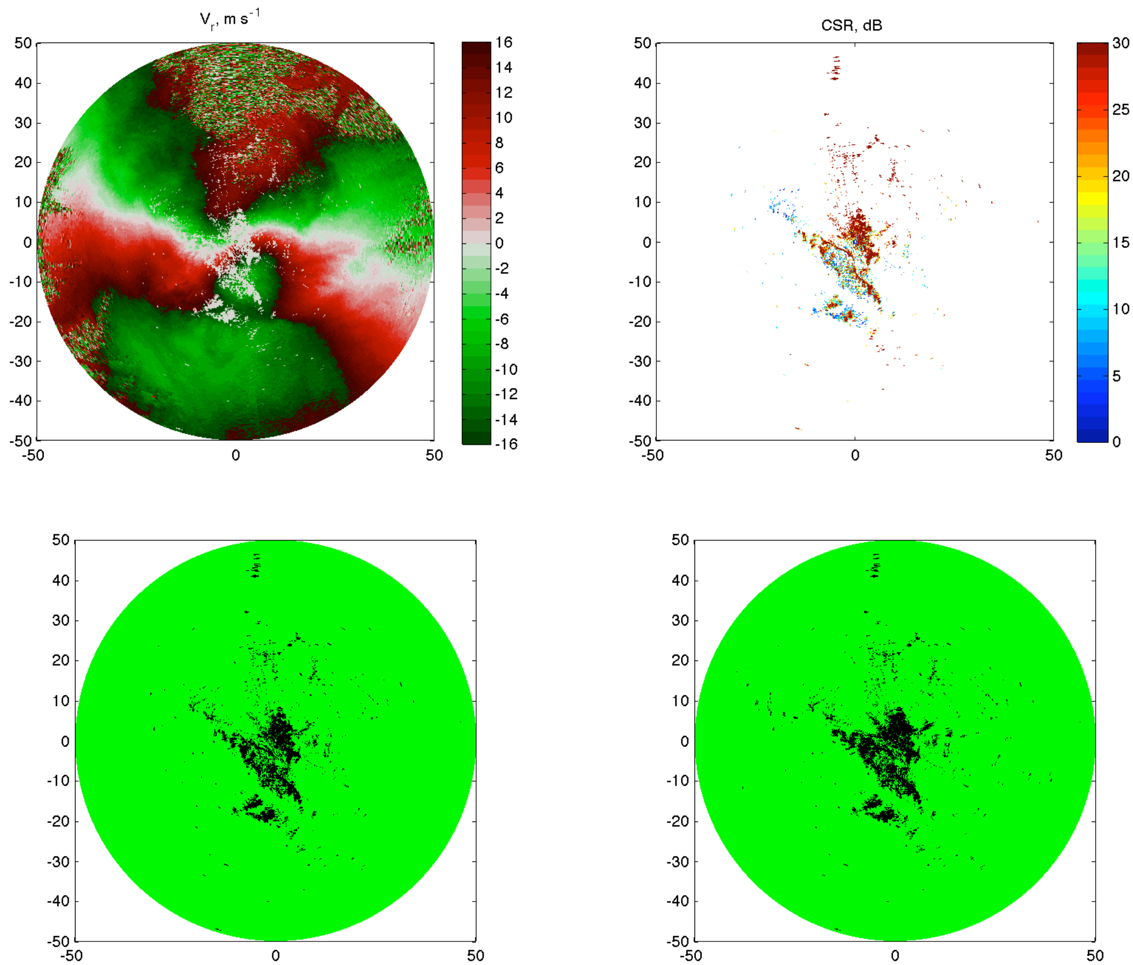

Fig. 5 Example of STEP processing (clutter identification): a) radial velocity; b) CSR; c) clutter truth; d) STEP identified clutter pixels (POD=97.5%, PFA=2.6%).

Fig. 6 compares the original moments of contamination (shown in the left column) with the results processed by STEP (shown in the right column). Four rows of figures, from top to bottom, give the results of radar reflectivity Z_H, radial velocity v_h, spectrum width σ_h, and correlation coefficient ρ_{hv}, respectively. For radar reflectivity, the clutter contamination is evident in the original result with a very high value while it is gone in the STEP result. For radial velocity, the bias is clearly seen in the original result while it disappears in the STEP result, which gives a smooth velocity field in the clutter region. For spectrum width, the original result shows larger values in the region of low SNR and smaller values in the clutter region. The STEP result reduces the estimation for the low SNR region and increases the estimation for the clutter region. The improved spectrum width image looks more smooth and consistent within the storm region. For correlation coefficient, lower values are shown for both clutter and low SNR regions in the original result. The values for these two regions have been increased in the STEP result, indicating that precipitation is present in these regions. Now the image of correlation coefficient is smooth enough that the radar echo can be easily classified as precipitation. From the example shown in Fig. 6, it is well demonstrated that the STEP algorithm can extensively improve the moment estimation for the application of polarimetric weather radar.

5. CONCLUSIONS

STEP is an advanced signal-processing framework that takes advantage of latest advances in clutter identification, filtering and moment estimation. The major feature of STEP algorithm is that it combines signal processing in both time and spectral domains, making it effective in mitigating clutter and noise effects on radar moment estimation. Compared to popular clutter filtering or moment estimation algorithms (e.g., CMD, GMAP, lag one estimator), the STEP algorithm adopts a more complex scheme and, therefore, requires more computational resources. This is a concern for the real-time implementation. As a result, further optimization and simplification work is on going. This work will be evaluated using EEC's operational modular radar processor (MRP) and tested with OU-PRIME.

ACKNOWLEDGEMENT

The study was partially supported by National Science Foundation Grant AGS-1046171 and EEC project "Spectrum-Time Estimation and Processing (STEP) for Weather Radar Signals". The authors are grateful of ARRC's research scientists and radar engineers in maintaining OU-PRIME radar and collecting radar data.

Reference:

Cao, Q., G. Zhang, R.D. Palmer, and L. Lei, 2011: Detection and Mitigation of Second Trip Echo in Polarimetric Weather Radar Measurements. *IEEE Transactions on Geoscience and Remote Sensing*, accepted and in press.

Cao, Q., G. Zhang, and R. Palmer, 2010: Real-time implementation of enhanced moment estimation on the C-band polarimetric research radar OU-PRIME. *ERAD 2010, The 6th European Conference on radar in Meteorology and Hydrology*, Sibiu, Romania, September 6-10, 2010.

Lei, L., G. Zhang, R.D. Palmer, B.L. Cheong, M. Xue, and Q. Cao, 2009: A multi-lag correlation estimator for polarimetric radar variables in the presence of noise, *AMS, 34th Conference on Radar Meteorology*, Williamsburg, VA, 5–9 October 2009

Li, Yinguang, G. Zhang, and R. Doviak, 2011: A new approach to detect the ground clutter mixed with weather echoes. Submitted to *J. Appl. Meteor. Climat.*, under review.

Palmer, R., D. Bodine, M. Kumjian, B. Cheong, G. Zhang, Q. Cao, H.B. Bluestein, A. Ryzhkov, T.-Y. Yu, and Y. Wang, 2011: Observations of the 10 May 2010 Tornado Outbreak in Central Oklahoma Using OU-PRIME: Potential for New Science with High-Resolution Polarimetric Radar, *Bulletin of the American Meteorological Society*, 92, 871-891.

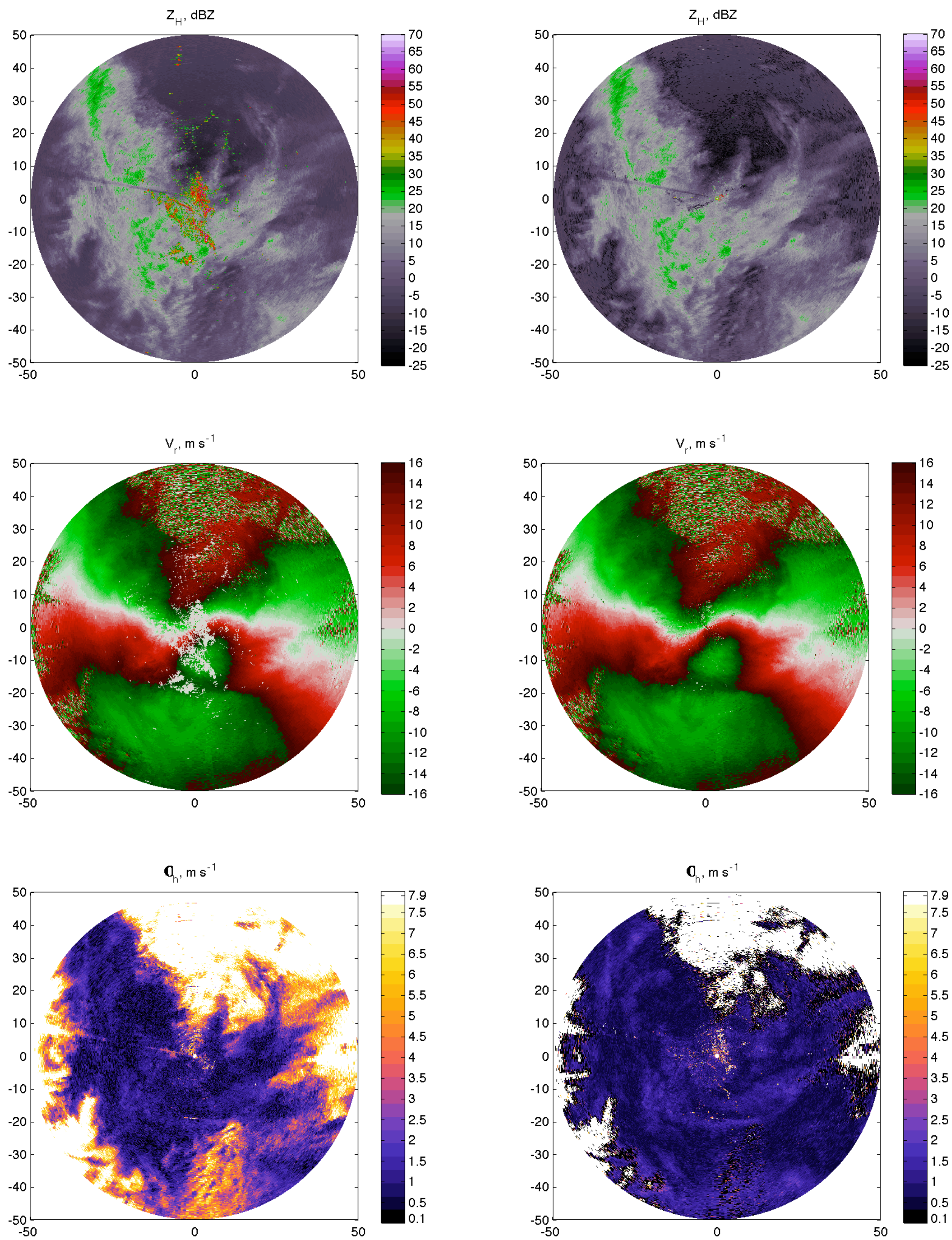
Z_H, dBZ
Z_H, dBZ
V_r, m s^{-1}
V_r, m s^{-1}
σ_h, m s^{-1}
σ_h, m s^{-1}

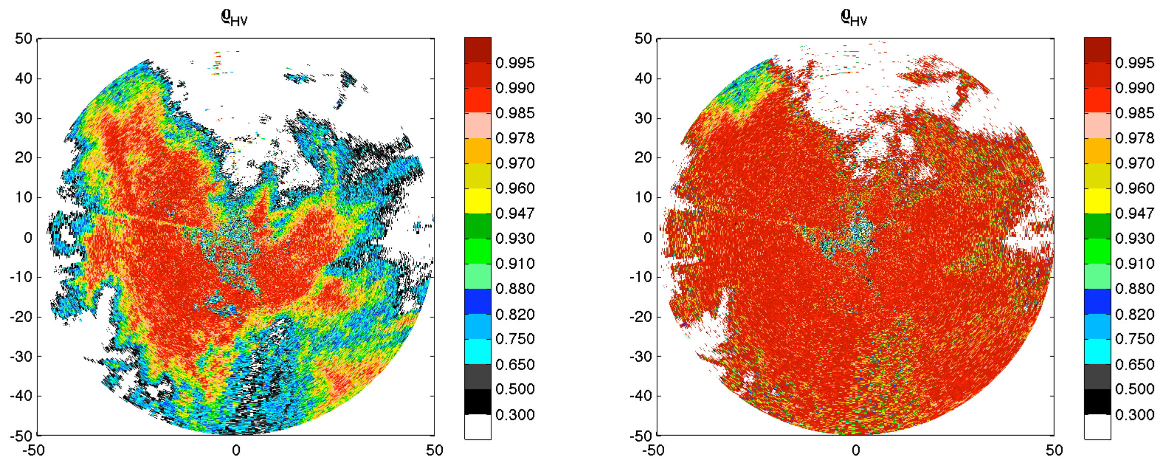

Fig. 6 Comparison of contaminated moments (left column) and STEP processed moments (right column). Four rows show radar reflectivity Z_H, radial velocity v_h, spectrum width σ_h, and correlation coefficient ρ_{hv}, respectively.